Proceedings of the Combustion Institute, Volume 28, 2000/pp. 2609–2618

FORMATION OF POLYCYCLIC AROMATIC HYDROCARBONS AND THEIR RADICALS IN A NEARLY SOOTING PREMIXED BENZENE FLAME

HENNING RICHTER, TIMOTHY G. BENISH, OLEG A. MAZYAR, WILLIAM H. GREEN AND JACK B. HOWARD

Department of Chemical Engineering
Massachusetts Institute of Technology
77 Massachusetts Avenue, Cambridge, MA 02139-4307, USA

Polycyclic aromatic hydrocarbons (PAH) are associated with health hazardous effects, and combustion processes are major sources of their presence in atmospheric aerosols. In the present work, chemical reaction pathways of PAH formation have been investigated by means of the modeling of a nearly sooting, low-pressure, premixed, laminar, one-dimensional benzene/oxygen/argon flame (equivalence ratio ϕ = 1.8, 30% argon, gas velocity at burner at 298 K v = 50 cm s^{-1}, pressure = 2.67 kPa). This flame has been investigated by Bittner and Howard using molecular-beam sampling coupled to mass spectrometry. More recently, Benish extended the set of available data for radicals up to 201 amu and for stable species up to 276 amu using nozzle-beam sampling followed by radical scavenging with dimethyl disulfide and subsequent analysis by gas chromatography–mass spectrometry. An existing kinetic model has been refined. Density functional theory computations were used to update the thermodynamic database, while transition state theory followed by a bimolecular quantum Rice-Ramsperger-Kassel analysis allowed for the determination of kinetic data relevant for the present study. The reaction of phenylacetylene radicals with acetylene is shown to be limiting for the concentration of 1-naphthyl radicals, while naphthalene is formed mainly by self-combination of cyclopentadienyl. The insufficient consumption of PAH as well as acetylene beyond the reaction zone gives some evidence of the need of additional PAH growth pathways involving acetylene but thermodynamically more favorable than subsequent hydrogen-abstraction/acetylene addition reactions. A new pathway for acenaphthylene formation is suggested and consists of benzyne recombination followed by hydrogen attack and isomerization.

Introduction

In epidemiological studies, air pollution has been positively associated with death from lung cancer and cardiopulmonary disease [1]. Combustion processes are major sources of airborne species of health concern; and a possible explanation of the health hazardous effect of atmospheric aerosols is their association with polycyclic aromatic hydrocarbons (PAH) [2]. Many PAH identified in aerosols have been found to be mutagenic [3], and their role as precursors of soot has been discussed [4,5]. Therefore, a better understanding of chemical reaction pathways leading to PAH formation is an essential issue in order to reduce their environmental impact and to improve combustion processes. Due to the complexity of such processes, the assessment of chemical reaction networks requires experiments in well-defined flow systems such as well-stirred reactors, plug-flow reactors, or premixed flames. Such systems allow the use of numerical modeling, taking into account sets of chemical reactions sufficiently large to describe individual reaction steps. Flame structures of laminar, premixed, fuel-rich, low-pressure flames have been measured by means of molecular-beam sampling coupled to mass spectrometry for different fuels such as acetylene [6] and benzene [6,7]. Molecular-beam sampling allows the measurement of radical intermediates, which is extremely valuable for the testing of kinetic models, but, unfortunately, sooting conditions are prohibitive for this technique. Probe sampling and subsequent analysis by gas chromatography coupled to mass spectrometry (GC-MS) allowed the measurement of concentration profiles for stable species up to coronene ($C_{24}H_{12}$) in premixed propane, acetylene, and benzene flames at reduced pressure [8], and up to pyrene ($C_{16}H_{10}$) in premixed methane, ethane, and propane flames at atmospheric pressure [9]. Concentration profiles of PAH up to ovalene ($C_{32}H_{14}$) and for the fullerenes C_{60}, C_{70}, C_{76}, C_{78}, and C_{84} have been measured using gas and liquid chromatography (GC-MS and HPLC) [10]. Detailed kinetic models describing PAH growth have been developed and tested for premixed methane [11], ethane [11], acetylene [12], and ethylene [12,13] flames.

The present work focuses on the detailed description of the first steps of the growth of PAH in a nearly sooting, low-pressure, premixed, laminar, one-dimensional benzene/oxygen/argon flame (equivalence

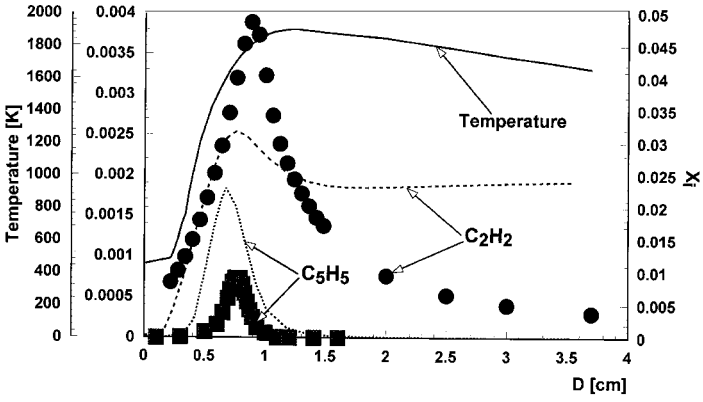

FIG. 1. Comparison between experimental mole fraction profiles and model predictions in a nearly sooting benzene/oxygen flame (ϕ = 1.8, 30% argon, v = 50 cm s^{-1}, 2.67 kPa). Temperature:—(experiment, [7]); C_2H_2: ● (experiment [7], right scale), ---- (prediction, right scale); C_5H_5: ■ (experiment [7], left scale), ··· (prediction, left scale.)

ratio ϕ = 1.8, 30% argon, gas velocity at burner at 298 K, v = 50 cm s^{-1}, pressure = 2.67 kPa) by means of kinetics modeling. This flame has been chosen because of the availability of a large set of experimental data and different modeling studies for comparison. Bittner and Howard [7] used molecular-beam sampling and measured concentration profiles for stable species up to 202 amu and radicals up to 91 amu. A temperature profile was obtained by means of thermocouple measurements, taking into account heat losses by radiation. The successful testing of the model for smaller stable and, in particular, radical intermediates involved in the growth process is essential for the confident application of a model to larger species and the assessment of potential errors and uncertainties.

Recently, the body of data available for Bittner and Howard's nearly sooting benzene flame was extended for radicals up to 201 amu and for stable species up to 276 amu [14], using nozzle beam sampling followed by radical scavenging with dimethyl disulfide (DMDS) and subsequent analysis by GC-MS [15]. This technique allowed for the identification of specific PAH radicals, that is, identification of the carbon site where hydrogen abstraction occurred, and their individual quantification using standard compounds for the analysis of the different scavenging products.

Oxidation chemistry of this flame has been studied by different authors using kinetic modeling [16–18]. The starting point of the present work was a recently published PAH model [19] which has been tested with encouraging results against Bittner and Howard's data [7], and also for a sooting, premixed benzene/oxygen/argon flame (ϕ = 2.4, 10% argon, v = 25 cm s^{-1}, p = 5.33 kPa) studied experimentally by Grieco et al. [10].

Approach

An existing kinetics model describing the formation of PAH [19] was refined and tested against the new set of experimental data measured recently by Benish [14] in a nearly sooting, low-pressure, premixed benzene/oxygen/argon flame using nozzle beam sampling followed by radical scavenging [15]. The computations were conducted with the PREMIX flame code [20] using an experimental temperature profile [7], shown in Fig. 1. Thermodynamic and kinetic data of the model were critically reviewed, updated if necessary, and completed. For instance, the formation of benzoquinone ($C_6H_4O_2$) [18,21] was added to the model. Subsequent benzoquinone pyrolysis and oxidation reactions [22] with acetylene and CO as major final products were implemented, as well as recent kinetic data on the consumption of cyclopentadiene [23] and cyclopentadienyl [24], the latter leading via unimolecular decay to C_2H_2 and C_3H_3. This addition of supplementary pathways for the consumption of cyclic C_6 and C_5 species and acetylene formation led in comparison to the initial model [19] to a significant improvement of the prediction capability for cyclopentadienyl, phenyl, and acetylene (Figs. 1 and 2). Possible reasons for the remaining overpredictions of cyclopentadienyl and phenyl are discussed later.

For species with unknown or poorly known thermodynamic properties, density functional theory calculations were carried out with the DGAUSS package [25] using the BLYP functional in conjunction with the DZVP basis set. The geometries were optimized, followed by determination of entropies and heat capacities after vibrational analysis. Heats of formation were taken from the NIST database [26] unless otherwise mentioned. For species for which no value was recommended, as was the case for most radical species, heats of formation were determined by means of isodesmic reaction, that is, reactions which maintain the overall number and types of bonds. The thermodynamic data of species involved in the studied chemical reaction pathways and deduced in the present work are given in Table 1; corresponding structures are shown in Table 2.

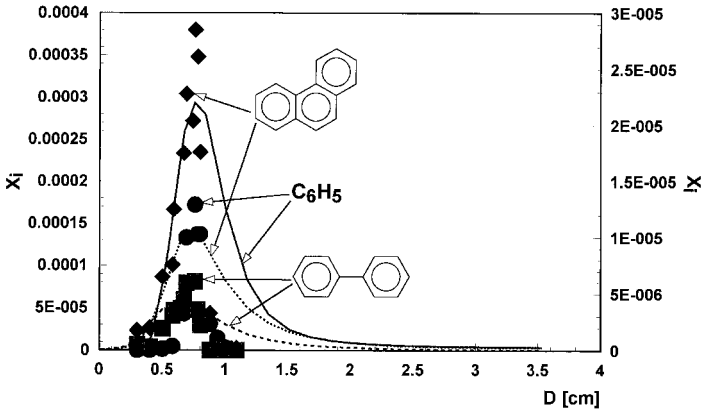

FIG. 2. Comparison between experimental mole fraction profiles and model predictions in a nearly sooting benzene/oxygen flame (ϕ = 1.8, 30% argon, v = 50 cm s^{-1}, 2.67 kPa). C_6H_5: ● (experiment [14], left scale), —— (prediction, left scale); biphenyl: ■ (experiment [14], left scale), ---- (prediction, left scale); phenanthrene: ◆ (experiment [14], right scale), ···· (prediction, right scale).

TABLE 1
Thermodynamic data of species used in the present work

Species	ΔH_f^0	S_f^0	$C_{p,\,300K}$	$C_{p,\,400K}$	$C_{p,\,500K}$	$C_{p,\,600K}$	$C_{p,\,800K}$	$C_{p,\,1000K}$	$C_{p,\,1500K}$
C_2H_2	54.19[a]	48.66	11.32	12.47	13.39	14.15	15.32	16.21	17.94
Cylcopentadienyl	62.56[b]	68.04	19.51	25.22	29.82	33.51	38.86	42.44	47.91
Cyclopentadiene	33.20[a]	65.87	18.74	25.19	30.49	34.85	41.36	45.82	52.40
Benzyne	103.39[c]	68.03	19.59	25.38	30.09	33.90	39.47	43.17	48.51
Phenyl	81.00[a]	68.00	19.90	26.50	31.89	36.26	42.69	46.99	53.22
Benzene	19.82[a]	64.58	20.23	27.45	33.40	38.28	45.54	50.49	57.71
$C_6H_5C_2H$*2	135.37[c]	82.29	29.05	36.16	41.93	46.59	53.39	57.91	64.48
Phenylacetylene	73.27[a]	81.64	29.81	37.48	43.74	48.84	56.37	61.46	69.04
Benzoquinone	−29.37[d]	76.79	26.17	32.91	38.40	42.86	49.37	53.67	59.69
1-Indenyl	65.01[c]	79.30	30.27	40.29	48.38	54.87	64.25	70.42	79.38
Indene	39.08[c]	80.88	30.57	41.07	49.67	56.67	67.01	73.95	83.96
$C_{10}H_6$-2	120.58[c]	81.88	32.08	41.80	49.71	56.11	65.45	71.58	80.16
1-Naphthyl	96.95[c]	83.16	32.29	42.91	51.54	58.52	68.67	75.36	84.84
2-Naphthyl	97.20[c]	83.07	32.35	42.97	51.59	58.56	68.71	75.39	84.87
Naphthalene	35.99[a]	80.40	32.66	43.93	53.14	60.61	71.59	78.90	89.36
1-$C_{10}H_7C_2H$*2	150.92[c]	94.23	40.77	52.04	61.16	68.49	79.10	86.06	96.04
2-$C_{10}H_7C_2H$*1	150.65[c]	95.36	41.01	52.23	61.30	68.60	79.15	86.09	96.04
1-$C_{10}H_7C_2H$	88.73[c]	94.63	41.35	53.26	62.93	70.76	82.16	89.71	100.58
2-$C_{10}H_7C_2H$	88.58[c]	93.60	41.44	53.33	62.98	70.78	82.14	89.68	100.58
Acenaphthylene	61.70[a]	86.62	37.50	50.37	60.81	69.22	81.39	89.36	100.56
Biphenylene	100.48[a]	87.77	37.81	50.54	60.88	69.23	81.35	89.31	100.52
Biphen-H	121.31[c]	92.03	39.74	53.10	63.94	72.68	85.35	93.68	105.52
Biphenyl*2	103.56[c]	95.60	40.03	53.26	63.95	72.55	85.04	93.35	105.44
Biphenyl	43.50[a]	93.27	40.45	54.24	65.46	74.55	87.90	96.88	109.93
1-Phenanthryl	109.20[c]	96.61	44.36	59.03	70.93	80.53	94.45	103.57	116.40
4-Phenanthryl	107.24[c]	96.44	44.41	59.10	71.02	80.63	94.57	103.69	116.46
Phenanthrene	48.09[a]	95.25	44.70	60.03	72.52	82.64	97.42	107.19	120.95

Note: ΔH_f^0 in kcal mol^{-1}; S_f^0, C_p in cal mol^{-1} K^{-1}.

[a] Heat of formation taken from the NIST database [26].

[b] Heat of formation taken from Moskaleva and Lin [24].

[c] Heat of formation calculated by means of isodesmic reaction.

[d] Heat of formation taken from Alzueta et al. [22].

[e] Heat of formation taken from Cox and Pilcher [27].

TABLE 2
Molecular structures of species used in the present work

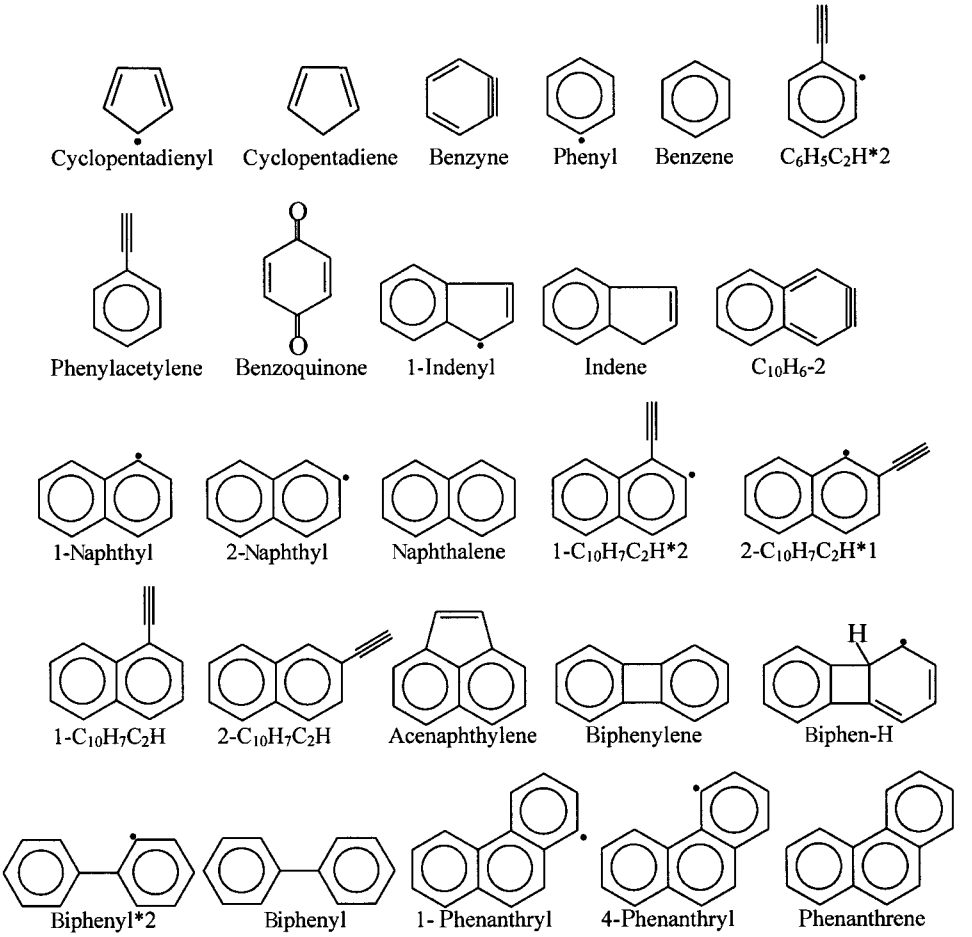

Kinetic data taken from the literature were adapted, if necessary, to low-pressure conditions by means of a bimolecular quantum Rice-Ramsperger-Kassel (QRRK) analysis [28]. The QRRK method used in the present work was significantly improved relative to prior studies by allowing multiple-well treatment and by approximating the distribution of the vibrational energy with three frequencies. In addition, a higher-order approximation was used for the efficiency factor of the stabilization of the chemically activated adduct via collision.

Taking into account the importance of these reactions in prior PAH models, a detailed analysis has been performed for acetylene-addition reactions to different PAH radicals. Only the reaction of phenyl with acetylene has been investigated experimentally, and only data at very low (about 0.1 Pa) [29] and atmospheric pressure [30] are available at temperatures relevant for the present study. Yu et al. [31] used transition state theory based on quantum-mechanical *ab initio* thermochemical and molecular structure data followed by a Rice-Ramsperger-Kassel-Markus (RRKM) treatment. The results could be quantitatively correlated with experimental data at different temperatures and pressures. Unfortunately, no data are available describing the effect of increasing radical size, and no rate constants have been determined for the case of possible formation of five-membered ring species such as acenaphthylene. For this reason, in the present work the potential energy surface of the reaction 1-naphthyl + acetylene has been explored using density functional theory, transition states have been identified, and high-pressure rate constants have been determined

TABLE 3
PAH growth reactions added or changed in the present work relative to ref. [19]

Reaction	k [$cm^3\ mol^{-1}\ s^{-1}$]	Ref.[a]
Benzene + H ⇆ phenyl + H_2	$3.23\ 10^{07}\ T^{2.095}\ \exp(-15842cal/RT)$	[35], p.w.[b]
Phenyl + H ⇆ benzene	$2.08\ 10^{30}\ T^{-4.98}\ \exp(-5290cal/RT)$	p.w., 2.67 kPa
Phenyl + H ⇆ benzyne + H_2	$1.18\ 10^{-6}T^{6.18}\ \exp(-4540cal/RT)$	p.w., 2.67 kPa
Phenyl + C_2H_2 ⇆ phenylacetylene + H	$9.33\ 10^{27}\ T^{-4.27}\ \exp(-17200cal/RT)$	p.w., 2.67 kPa
Phenylacetylene + H ⇆ $C_6H_5C_2H$*2 + H_2	$3.23\ 10^{07}\ T^{2.095}\ \exp(-15842cal/RT)$	[35], p.w.[b]
$C_6H_5C_2H$*2 + H ⇆ phenylacetylene	$9.64\ 10^{30}\ T^{-5.07}\ \exp(-7800cal/RT)$	p.w., 2.67 kPa
$C_6H_5C_2H$*2 + C_2H_2 ⇆ 1-naphthyl	$1.40\ 10^{05}\ T^{2.282}\ \exp(-3261cal/RT)$	p.w.[c]
1-Naphthyl + H ⇆ naphthalene	$1.19\ 10^{26}\ T^{-3.75}\ \exp(-4070cal/RT)$	p.w., 2.67 kPa
2-Cyclopentadienyl ⇆ naphthalene + 2 H	$2.00\ 10^{13}\ \exp(-8000cal/RT)$	[32]
Naphthalene + H ⇆ 1-naphthyl + H_2	$3.23\ 10^{07}\ T^{2.095}\ \exp(-15842cal/RT)$	[35], p.w.[b]
Naphthalene + H ⇆ 2-naphthyl + H_2	$3.23\ 10^{07}\ T^{2.095}\ \exp(-15842cal/RT)$	[35], p.w.[b]
2-Naphthyl + H ⇆ naphthalene	$1.67\ 10^{26}\ T^{-3.80}\ \exp(-4110cal/RT)$	p.w., 2.67 kPa
2-Naphthyl + H ⇆ $C_{10}H_6$-2 + H_2	$2.76\ 10^{-23}\ T^{11.08}\ \exp(-5960cal/RT)$	p.w., 2.67 kPa
1-Naphthyl + C_2H_2 ⇆ 1-$C_{10}H_7C_2H$ + H	$1.84\ 10^{-4}\ T^{5.02}\ \exp(-10350cal/RT)$	p.w., 2.67 kPa
1-Naphthyl + C_2H_2 ⇆ acenaphthylene + H	$8.54\ 10^{22}\ T^{-2.849}\ \exp(-11370cal/RT)$	p.w., 2.67 kPa
2 Benzene ⇆ biphenylene	$4.60\ 10^{12}$	[37]
Biphenylene + H ⇆ biphen-H	$4.04\ 10^{13}\ \exp(-4300cal/RT)$	[35], p.w.[b]
Biphen-H ⇆ acenaphthylene + H	$1.00\ 10^{13}\ \exp(-20000cal/RT)$	p.w.[b]
2-Naphthyl + C_2H_2 ⇆ 2-$C_{10}H_7C_2H$ + H	$2.68\ 10^{27}\ T^{-4.09}\ \exp(-20100cal/RT)$	p.w., 2.67 kPa
1-$C_{10}H_7C_2H$ + H ⇆ 1-$C_{10}H_7C_2H$*2 + H_2	$3.23\ 10^{07}\ T^{2.095}\ \exp(-15842cal/RT)$	[35], p.w.[b]
2-$C_{10}H_7C_2H$ + H ⇆ 2-$C_{10}H_7C_2H$*1 + H_2	$3.23\ 10^{07}\ T^{2.095}\ \exp(-15842cal/RT)$	[35], p.w.[b]
1-$C_{10}H_7C_2H$*2 + C_2H_2 ⇆ 4-phenanthryl	$1.40\ 10^{05}\ T^{2.282}\ \exp(-3261cal/RT)$	p.w.[c]
2-$C_{10}H_7C_2H$*1 + C_2H_2 ⇆ 1-phenanthryl	$1.40\ 10^{05}\ T^{2.282}\ \exp(-3261cal/RT)$	p.w.[c]
1-Phenanthryl + H ⇆ phenanthrene	$5.00\ 10^{13}$	[19]
4-Phenanthryl + H ⇆ phenanthrene	$5.00\ 10^{13}$	[19]
Phenyl + phenyl ⇆ biphenyl	$9.87\ 10^{26}\ T^{-4.30}\ \exp(-4610cal/RT)$	[33], p.w.[b]
Biphenyl + H ⇆ biphenyl*2 + H_2	$3.23\ 10^{07}\ T^{2.095}\ \exp(-15842cal/RT)$	[35], p.w.[b]
Biphenyl*2 + C_2H_2 ⇆ phenanthrene + H	$1.40\ 10^{05}\ T^{2.282}\ \exp(-3261cal/RT)$	p.w.[d]
1-Indenyl + cyclopentadienyl ⇆ phenanthrene + 2 H	$1.00\ 10^{13}\ \exp(-8000\ cal/RT)$	[32]

[a] p.w., present work.
[b] See text.
[c] 0.25 × high pressure limit determined for 1-naphthyl + C_2H_2.
[d] High pressure limit determined for 1-naphthyl + C_2H_2.

without any empirical adjustments. Finally, bimolecular QRRK treatment at different temperatures and pressures allowed the determination of rate constants of the reactions of 1-naphthyl with acetylene forming different products such as 1-naphthylacetylene or acenaphthylene. In order to assess its reliability, the same approach was used for phenyl + acetylene and yielded results very close to the experimental high-temperature data measured by Fahr and Stein [29] and Heckmann et al. [30]. The potential energy surfaces of phenyl + acetylene and 1-naphthyl + acetylene appeared to be very similar except for the possibility of the formation of five-membered rings in the latter case. Therefore, rate constants for 2-naphthyl + acetylene leading to 2-naphthylacetylene or the corresponding adduct were deduced via a bimolecular QRRK treatment using the same high-pressure rate constants as in the 1-naphthyl case, but without allowing for the formation of five-membered rings. The rate constants deduced for 2.67 kPa and used in this work are included in Table 3.

Results

Formation of Naphthalene

Mainly, two possible pathways for the formation of naphthalene have been suggested in the past and are included in the present model. Wang and Frenklach [12] identified hydrogen abstraction–acetylene addition to be sufficient for naphthalene formation in premixed acetylene and ethylene flames and

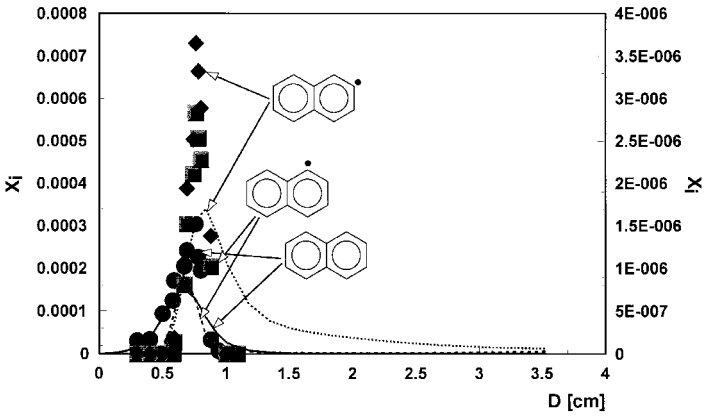

FIG. 3. Comparison between experimental mole fraction profiles and model predictions in a nearly sooting benzene/oxygen flame (ϕ = 1.8, 30% argon, v = 50 cm s^{-1}, 2.67 kPa). Naphthalene: ● (experiment [14], left scale), —— (prediction, left scale); 1-naphthyl: ■ (experiment [14], right scale), ---- (prediction, right scale); 2-naphthyl: ◆ (experiment [14], right scale), ··· (prediction, right scale).

pointed out the importance of thermodynamics in PAH growth. In other studies [11,13], naphthalene production has been accounted for by resonantly stabilized cyclopentadienyl self-combination, which is used here with the updated rate constant suggested by Marinov et al. [32]. A good agreement with experimental data was obtained (Fig. 3), and prior results [19] showing cyclopentadienyl self-combination to be the major pathway to naphthalene in benzene flames have been confirmed. In the present study, even if the high-pressure limit determined for 1-naphthyl + acetylene is used as the rate constant, the ring closure reaction leading from acetylene and phenylacetylene radical to 1-naphthyl is too slow. The sole use of this reaction gives a naphthalene peak mole fraction which is more than 1 order of magnitude smaller than the experimental value, despite a twofold overprediction of the phenylacetylene peak mole fraction, resulting from the propagation of the phenyl overprediction mentioned above. The omission of the reaction of acetylene with phenylacetylene radical affected the naphthalene concentration profiles only in the postflame zone where a mole fraction of approximately 1×10^{-5} instead of approximately 1×10^{-6} persisted. The comparison of model predictions with experimental mole fraction profiles for 1-naphthyl and 2-naphthyl [14], shown in Fig. 3, led to the conclusion that the concentration of 1-naphthyl is mainly determined by the equilibrium constant of the reaction of the phenylacetylene radical (A1C2H*2) with acetylene. The fluxes of the forward and reverse reactions are tightly balanced [12], and the concentration of 1-naphthyl is found to be very sensitive to the rate constant chosen for this reaction. Only the presence of ring closure via the reaction of acetylene with the phenylacetylene radical provided an explanation for the 1-naphthyl concentration being significantly lower than that of 2-naphthyl as found experimentally. The more pronounced underprediction for 1-naphthyl compared to that of 2-naphthyl reflects insufficient knowledge of the rate constant for ring closure via acetylene attack on PAH-C_2H radicals, but may be also attributed partially to the uncertainty of related thermodynamic data. The sole use of the reaction of acetylene with phenylacetylene radical (without cyclopentadienyl self-combination) leads to a reduction of the peak mole fraction of 1-naphthyl by ≈35%, keeping a similar shape as that shown in Fig. 3. A much stronger impact of the removal of cyclopentadienyl self-combination was observed for 2-naphthyl. Compared to the profile shown in Fig. 3, the predicted peak value decreased by nearly 1 order of magnitude and shifted by about 7 mm toward the postflame zone. The results for naphthalene and its radicals indicate that both cyclopentadienyl self-combination and hydrogen abstraction–acetylene addition play roles in the formation of the second aromatic ring.

Formation of Biphenyl and Phenanthrene

Biphenyl is formed via the recombination of phenyl radicals (Fig. 2). Due to chemical activation, the competition between forward and reverse reactions is pressure dependent. The rate constant for biphenyl formation at 2.67 kPa was determined using a QRRK treatment [28] and the expression suggested by Park and Lin [33] for the high-pressure limit. The reaction of phenyl with benzene [34] has been included in the model but did not contribute significantly to biphenyl formation due to an unfavorable thermodynamic equilibrium.

Hydrogen abstraction from biphenyl followed by acetylene attack and ring closure has been shown to be the main phenanthrene formation pathway in the reaction zone of a premixed acetylene flame [12] and to be the sole significant source of phenanthrene in benzene flames [19]. Phenanthrene formation via the fusion of two five-membered rings in the reaction of indenyl with cyclopentadienyl [11,13,32], similar to naphthalene formation by cyclopentadienyl self-combination, is also included in the present model. However, it contributes only about 15%

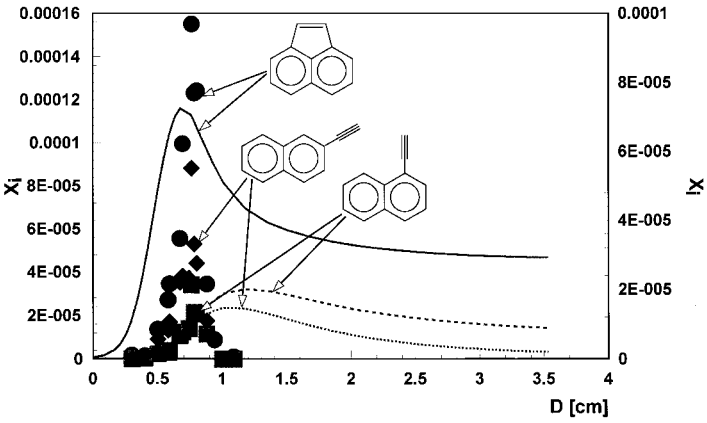

FIG. 4. Comparison between experimental mole fraction profiles and model predictions in a nearly sooting benzene/oxygen flame (ϕ = 1.8, 30% argon, v = 50 cm s^{-1}, 2.67 kPa). Acenaphthylene: ● (experiment [14], left scale), —— (prediction, left scale); 1-naphthylacetylene: ■ (experiment [14], right scale), ---- (prediction, right scale); 2-naphthylacetylene: ◆ (experiment [14], right, scale), ··· (prediction, right scale).

of the peak mole fraction and plays no significant role close to the burner and in the postflame zone. Peak locations of the biphenyl and phenanthrene profiles correspond well with experimental data [14], but the peak value of phenanthrene is underpredicted by a factor of 2 to 3 (Fig. 2). In agreement with the rate analysis of Wang and Frenklach [12], the reverse reaction of ring closure via acetylene reaction with naphthylacetylene radicals is largely responsible for the decreasing mole fraction of phenanthrene beyond the reaction zone. Therefore, removal of the ring closure reaction leads to a two-fold increase of the peak value and a more pronounced lack of consumption in the postflame zone. The sole use of two subsequent hydrogen abstraction–acetylene addition steps for phenanthrene formation leads to an underprediction of 2 to 3 orders of magnitude. The 1- and 2-naphthylacetylene mole fraction profiles have been measured by Benish [14], and the model shows good agreement for the peak value of 1-naphthylacetylene and a two- to four-fold underprediction for its isomer (Fig. 4). The slight shift of the predicted 2-naphthylacetylene profile toward the postflame zone may indicate that the predicted rate of naphthylacetylene formation is too slow. This observation could reflect an uncertainty in kinetic data or the presence of other formation pathways. Both naphthylacetylene isomers persist with significant concentrations in the burned gases, an additional indication of the thermodynamic limitations of ring closure after hydrogen abstraction and subsequent reaction with acetylene. The rate constant used for all hydrogen-abstraction reactions was calculated for a temperature range from 300 to 2100 K using the thermodynamic data presented in Table 1 and the $C_6H_5 + H_2$ reaction rate constant determined by Mebel et al. [35]. The resulting rate constant is in excellent agreement with the high-temperature data of Kiefer et al. [36], which have been used previously [19].

Formation of Acenaphthylene

Acenaphthylene has been significantly underpredicted in prior modeling studies [11,13,19,32] using acetylene attack on 1-naphthyl followed by ring closure and hydrogen loss. Hausmann et al. [15] suggested the necessity of additional acenaphthylene-forming reactions based on the experimentally measured structure of a premixed benzene flame. In the present study, the sole use of acetylene attack on 1-naphthyl and using a rate constant determined by QRRK (Table 3) led to a 50-fold underprediction compared to the peak value measured by Benish [14]. The latter is about 3 to 5 times higher than the value previously obtained by Bittner and Howard [7] using molecular-beam sampling coupled to mass spectrometry. This discrepancy is believed to reflect the uncertainty of mass spectrometric detection without direct calibration with standards of known concentration. Taking into account the careful quantification conducted by Benish [14], the mole fraction profile measured by means of GC-MS must be considered to be more reliable and is used in the present study.

The first step in the development of an additional acenaphthylene formation pathway was the detection of biphenylene, an isomer of acenaphthylene, in the work of Benish [14]. Biphenylene formation by recombination of benzyne has been measured [37] and is included in the present model. Benzyne (C_6H_4) is formed mainly by hydrogen abstraction from phenyl. A QRRK computation was carried out in order to take into account the pressure dependence of this reaction due to its competition with recombination to benzene. Besides benzyne dimerization, its isomerization to the corresponding linear species and decomposition to acetylene and diacetylene (C_4H_2), as suggested by Moskaleva et al. [38], were used in the present study. The sum of the peak concentrations of benzyne and linear C_6H_4 predicted by the present model is about 3.5 times larger

than the experimental C_6H_4 peak value measured by Bittner and Howard [7] using mass spectrometry. The predicted benzyne peak concentration was close to 50% higher than that of linear C_6H_4. Peak location and shape of the profiles are in good agreement; the discrepancy in the absolute values can be attributed to a propagation of the phenyl overprediction but also to possible additional consumption pathways such as reaction with larger benzyne-type species.

Motivated by results of Necula and Scott [39], the possible isomerization of biphenylene to acenaphthylene has been investigated by means of pyrolysis experiments conducted at temperatures up to 1100 °C [40]. In apparent contradiction to the idea of isomerization, unreacted biphenylene remained the dominant compound even at 1100 °C, and only traces of acenaphthylene could be detected. However, pyrolysis of 2-bromobiphenyl yielded acenaphthylene as the major product at 1100 °C, while at 800 °C only traces were detected. These data led us to assume tentatively the occurrence of ring closure to a biphenylene-H species which isomerizes to the thermodynamically more favorable corresponding acenaphthylene-H species followed by hydrogen loss.

Based on these results and the significant mole fraction of hydrogen radicals (up to approximately 0.01), the formation of the biphenylene-H species via hydrogen addition to biphenylene followed by isomerization was included in the model. The rate constant suggested by Mebel et al. [35] for hydrogen addition to benzene was used due to its similarity to the corresponding biphenylene reaction (i.e., the destruction of an aromatic ring system), while the rate constant of the isomerization had to be estimated. An acenaphthylene peak mole fraction of about 75% of the experimental one (Fig. 4) was predicted, indicative of a major role of the biphenylene pathway. Using the rate constants presented in Table 3, the shape of the biphenylene mole fraction profile agrees with the experimental findings and shows a nearly complete consumption after its peak in the reaction zone. The peak is overpredicted 10-fold, but its value depends strongly on the choice of the rate constants for hydrogen addition and isomerization. A 10-fold increase of the hydrogen addition rate constant reduces the biphenylene overprediction to less than 75% and leads to a nearly perfect match of the predicted and experimental peak values of acenaphthylene. Other possible reasons for the biphenylene overprediction may be the propagation of the benzyne overprediction or the decrease of the dimerization rate constant at flame temperatures. The dimerization rate constant was determined between 90 and 200 °C, and no activation energy was observed [37]. However, at higher temperatures, chemical activation of the dimer could enhance the reverse reaction to benzyne, compared to the stabilization of biphenylene. Due to large uncertainties in the rate constants, no further adjustment has been made, and more work will be necessary for an exact quantitative description of the suggested pathway.

Similar pathways for the formation other PAH are conceivable, and therefore the formation of a benzyne-type two-membered ring species ($C_{10}H_6$-2, Table 2) has been tested. The similarity of the predicted mole fraction with the results obtained by Bittner and Howard [7] for $C_{10}H_6$ species is encouraging, and further exploration of the role of biphenylene-type species as intermediates in PAH formation seems to be promising.

Acenaphthylene is consumed in the present model via hydrogen abstraction at all radical sites followed by reactions with acetylene. The predicted decay is significantly too slow beyond the reaction zone (Fig. 4), indicating the necessity of additional efficient PAH consumption reactions.

Conclusions

An existing kinetic model describing the formation of PAH was updated and improved. Recently published kinetic data describing the oxidation of six- and five-membered ring species were implemented, and thermodynamic data for key species involved in the growth process were determined using *ab initio* quantum-mechanical computations. Different radical sites could be distinguished. The kinetics of acetylene addition to PAH radicals was deduced by means of transition state theory, and the relative importance of ring closure leading to five-membered ring species such as acenaphthylene was determined. A QRRK treatment allowed the computation of rate constants at the pressure used in the present study. The prediction of the kinetic model has been tested against experimental data from a nearly sooting, low-pressure, premixed benzene/oxygen/argon flame. The set of experimental data included mole fraction profiles of radical species measured by means of radical scavening with dimethyl disulfide followed by GC-MS analysis. The use of reliable thermodynamic and kinetic data but also the availability of experimental concentration profiles of intermediate, often radical, species increased significantly the level of confidence in conclusions about reaction pathways and their elementary reactions responsible for PAH growth. The importance of thermodynamic limitations of PAH growth via hydrogen abstraction–acetylene addition sequences has been shown. Ring closure via the reaction of PAH-C_2H radicals with acetylene was shown to be a net consumption pathway of naphthalene, phenanthrene, and corresponding radicals. A general feature of the model prediction is that the consumption of PAH-C_2H species is too slow compared to the experimental data. This observation, the underprediction of larger PAH, not discussed here, as well as the lack

of acetylene consumption beyond the reaction zone, indicates the necessity of additional thermodynamically favorable PAH growth and acetylene consumption pathways. The important contribution of cyclopentadienyl and phenyl has been shown for the formation of naphthalene and phenanthrene (via biphenyl), and also for benzo[b]fluoranthene, not discussed here. The implication of these radicals in the formation of larger PAH which are not considered in the present model may be an explanation for the overprediction of these radicals. A reaction sequence leading from benzyne dimerization and isomerization to acenaphthylene has been tested with encouraging results. The participation of benzyne-type species seems to be promising and will be investigated in future work.

Acknowledgments

Different parts of this research were supported by the Chemical Sciences Division, Office of Basic Energy Sciences, Office of Energy Research, U.S. Department of Energy under grant DE-FGO2-84ER13282; the National Institute of Environmental Health Sciences Center grant NIH-5P30-ES02109; and the National Aeronautics and Space Administration under grant NAG3-1879. The authors thank Prof. J. W. Bozzelli from the New Jersey Institute of Technology for providing software and valuable advice.

REFERENCES

1. Dockery, D. W., Pope, C. A., Xu, X., Spengler, J. D., Ware, J. H., Fay, M. E., Ferris, B. G., and Speizer, F. E., *N. Engl. J. Med.* 329:1753–1759 (1993).
2. Allen, J. O., Dookeran, N. M., Smith, K. A., Sarofim, A. F., Taghizadeh, K., and Lafleur, A. L., *Environ. Sci. Technol.* 30:1023–1031 (1996).
3. Durant, J. L., Busby, W. F., Lafleur, A. L., Penman, B. W., and Crespi, C. L., *Mutat. Res.* 371:123–157 (1996).
4. Haynes, B. S., and Wagner, H. Gg., *Prog. Energy Combust. Sci.* 7:229–273 (1981).
5. Frenklach, M., Clary, D. W., Gardiner, W. C., and Stein, S. E., *Proc. Combust. Inst.* 20:887–901 (1984).
6. Homann, K. H., and Wagner, H. Gg., *Proc. Combust. Inst.* 11:371–379 (1967).
7. Bittner, J. D., and Howard, J. B., *Proc. Combust. Inst.* 18:1105–1116 (1980).
8. Bockhorn, H., Fetting, F., and Wenz, H. W., *Ber. Bunsen-Ges. Phys. Chem.* 87:1067–1073 (1983).
9. Senkan, S., and Castaldi, M., *Combust. Flame* 107:141–150 (1996).
10. Grieco, W. J., Lafleur, A. L., Swallow, K. C., Richter, H., Taghizadeh, K., and Howard, J. B., *Proc. Combust. Inst.* 27:1669–1675 (1998).
11. Marinov, N. M., Pitz, W. J., Westbrook, C. K., Castaldi, M. J., and Senkan, S. M., *Combust. Sci. Technol.* 116–117:211–287 (1996).
12. Wang, H., and Frenklach, M., *Combust. Flame* 110:173–221 (1997).
13. Castaldi, M. J., Marinov, N. M., Melius, C. F., Huang, J., Senkan, S. M., Pitz, W. J., and Westbrook, C. K., *Proc. Combust. Inst.* 26:693–702 (1996).
14. Benish, T. G., "PAH Radical Scavenging in Fuel-Rich Premixed Benzene Flames," Ph.D. thesis, Massachusetts Institute of Technology, Cambridge, MA, 1999.
15. Hausmann, H., Hebgen, P., and Homann, K.-H., *Proc. Combust. Inst.* 24:793–801 (1992).
16. Lindstedt, R. P., and Skevis, G., *Combust. Flame* 99:551–561 (1994).
17. Zhang, H.-Y., and McKinnon, J. T., *Combust. Sci. Technol.* 107:261–300 (1995).
18. Tan, F., and Frank, P., *Proc. Combust. Inst.* 26:677–684 (1996).
19. Richter, H., Grieco, W. J., and Howard, J. B., *Combust. Flame* 119:1–22 (1999).
20. Kee, R. J., Grcar, J. F., Smooke, M. D., and Miller, J. A., *A FORTRAN Program for Modeling Steady Laminar One-Dimensional Premixed Flames,* Sandia report SAND85-8240, 1997.
21. Yu, T., and Lin, M. C., *J. Am. Chem. Soc.* 116:9571–9576 (1994).
22. Alzueta, M. U., Oliva, M., and Glarborg, P., *Int. J. Chem. Kinet.* 30:683–697 (1998).
23. Roy, K., Horn, C., Frank, P., Slutsky, V. G., and Just, T., *Proc. Combust. Inst.* 27:329–336 (1998).
24. Moskaleva, L. V., and Lin, M. C., "Unimolecular Isomerization/Decomposition of Cyclopentadienyl and Related Bimolecular Reverse Process: Ab Initio MO/Statistical Theory Study," *J. Comput. Chem.,* 21:415–425 (2000).
25. Unichem 4.0, Chemistry Codes UC-5505 4.0, Oxford Molecular Group, PLC, Beaverton, OR, 1997.
26. Afeefy, H. F., Liebman, J. F., Stein, S. E., "Neutral Thermochemical Data," in *NIST Chemistry Web Book, NIST Standard Reference Database Number 69* (W. G. Mallard and P. J. Lindstrom, eds.), National Institute of Standards and Technology, Gaithersburg, MD, February 2000 (http://webbook.nist.gov).
27. Cox, J. D., and Pilcher, G., *Thermochemistry of Organic and Organometallic Compounds,* Academic Press, London, 1970, pp. 166–167.
28. Dean, A. M., Bozzelli, J. W., and Ritter, E. R., *Combust. Sci. Technol.* 80:63–85 (1991).
29. Fahr, A., and Stein, S. E., *Proc. Combust. Inst.* 22:1023–1029 (1988).
30. Heckmann, E., Hippler, H., and Troe, J., *Proc. Combust. Inst.* 26:543–550 (1996).
31. Yu, T., Lin, M. C., and Melius, C., *Int. J. Chem. Kinet.* 26:1095–1104 (1994).
32. Marinov, N. M., Pitz, W. J., Westbrook, C. K., Vincitore, A. M., Castaldi, M. J., Senkan, S. M., and Melius, C. F., *Combust. Flame* 114:192–213 (1998).
33. Park, J., and Lin, M. C., *J. Phys. Chem. A* 101:14–18 (1997).
34. Park, J., Burova, S., Rodgers, A. S., and Lin, M. C., *J. Phys. Chem. A* 103:9036–9041 (1999).

35. Mebel, A. M., Lin, M. C., Yu, T., and Morokuma, K., *J. Phys. Chem. A* 101:3189–3196 (1997).
36. Kiefer, J. H., Mizerka, L. J., Patel, M. R., and Wei, H.-C., *J. Phys. Chem.* 89:2013–2019 (1985).
37. Porter, G., and Steinfeld, J. I., *J. Chem. Soc. A* 877–878 (1968).
38. Moskaleva, L. V., Madden, L. K., and Lin, M. C., *Phys. Chem. Chem. Phys.* 1:3967–3972 (1999).
39. Necula, A., and Scott, L. T., Boston College, personal communication, 1999.
40. Risoul, V., Massachusetts Institute of Technology, unpublished data, 1999.

COMMENTS

Christopher Pope, Sandia National Laboratories, USA. I just wanted to comment that our recent modeling results [1] show similar behavior with regard to the HACA mechanism. While not mentioned in our talk, the main formation pathway for naphthalene was the combination of two cyclopentadienyl radicals with the (C_8H_5) *o*-ethynyl phenyl + $C_8H_8 \rightarrow$ ($C_{10}H_7$) 1-naphthyl reaction being a naphthyl decomposition pathway for the C_2H_4 + propene (C_3H_6) flames modeled. However, in the C_2H_2 flame, the C_8H_5 + $C_2H_2 \rightarrow C_{10}H_7$ reaction was the major pathway for naphthalene formation, with $2C_5H_5 \rightarrow C_{10}H_8$ being of minor importance. Similarly, the *n*-C_4H_3 + $C_2H_2 \rightarrow$ (C_6H_5) phenyl reaction was a major phenyl decomposition channel for the C_2H_4 + C_3H_6 flames.

So, for low pressure flames in which C_2H_2 is not the fuel, I see a similar picture emerging. I suspect that much of why the HACA reactions are going in reverse is the effect of pressure on the equilibrium constant, which would cause such combination reactions of two species becoming one to be much less favored. (This also might provide a partial explanation for the major products of $2C_3H_3$ to be C_6H_5 + H at low pressures.)

There is therefore the real possibility that the HACA reactions might become more important at higher pressures to what extent remains to be seen.

REFERENCE

1. Pope, C. J., and Miller, J. A., *Proc. Combust. Inst.* 28:1519–1527 (2000).

Author's Reply. The authors thank Dr. Pope for the additional information. The finding that relative contributions of different pathways to PAH growth and consumption depend on the fuel is consistent with PAH growth reactions being tightly balanced. Therefore, the careful choice of thermodynamic data used for kinetic modeling is essential. Pronounced sensitivity to experimental conditions of the contribution of subsequent hydrogen-abstraction/acetylene-addition steps to naphthalene formation has also been observed in our work on the modeling of combustion in a coupled well-stirred/plug-flow reactor system [1] using the reaction mechanism of the present work adapted for atmospheric pressure. HACA sequences are nearly solely responsible for naphthalene formation in the case of ethylene combustion while benzene combustion showed characteristics similar to the low pressure premixed benzene flame investigated in the present work, that is, naphthalene formation via cyclopentadienyl combination.

Our different finding for naphthalene formation in ethylene flames as compared to Dr. Pope's work might be related to the pressure-dependence of the equilibrium corresponding to the HACA mechanism, as pointed out in the comment, but also to the temperature of the aforementioned study, which is 1620 K, significantly lower than the maximum temperature of the flame investigated by Dr. Pope (2208 K). The equilibrium constant corresponding to PAH growth via the HACA mechanism decreases significantly with increasing temperature due to the entropy effect of a decreasing number of molecules.

REFERENCE

1. Marr, J. A., "PAH Chemistry in a Jet-Stirred/Plug-Flow Reactor System", Ph.D. thesis, Massachusetts Institute of Technology, 1993.